ELSEVIER

Coastal Engineering 36 (1999) 219–242

COASTAL ENGINEERING

Simulation and prediction of swash oscillations on a steep beach

T.E. Baldock *, P. Holmes

Department of Civil Engineering, Imperial College of Science, Technology and Medicine, London, SW7 2BU, UK

Received 10 March 1998; received in revised form 2 February 1999; accepted 2 February 1999

Abstract

This paper presents numerical simulations and analytical predictions of key aspects of swash oscillations on a steep beach. Simulations of the shoreline displacement based on bore run-up theory are found to give excellent agreement with recent experimental data for regular waves, wave groups and random waves. The theory is used to derive parameters that predict the onset of swash saturation and the spectral characteristics of the saturated shoreline motion. These parameters are again in good agreement with the measured laboratory data and are also consistent with previous experimental data. Simulation of irregular wave run-up using a series of overlapping monochromatic swash events is found to reproduce typical features of swash oscillations and can accurately describe both the low and high frequency spectral characteristics of the swash zone. In particular, the low frequency components of the run-up can be modelled directly using a sequence of incident short wave bores, with no direct long wave input to the numerical simulations. This suggests that wave groupiness must be accounted for when modelling shoreline oscillations.

Keywords: Swash; Run-up; Bores; Wave grouping; Random waves; Beaches

1. Introduction

Wave run-up and run-down (or swash) is one of the principal factors affecting the stability of natural beaches and coastal structures. In particular, beach morphology is

* Corresponding author. School of Civil and Structural Engineering, University of Plymouth, Palace St., Plymouth, PL1 2DE, UK. Tel.: +44-1752-233-664; Fax: +44-1715-233-658; E-mail: t.baldock@plymouth.ac.uk

0378-3839/99/$ - see front matter
PII: S0378-3839(99)00011-3

strongly influenced by the nature of the swash zone, both over short (storm) durations and longer time scales (Wright and Short, 1984; Hughes, 1992). Predicting and modelling swash zone processes is therefore critical for understanding beach behaviour and the forces on structures in the coastal zone (Hamm et al., 1993).

This paper considers this point and presents numerical simulations and analytical predictions for both regular and irregular wave run-up. The bore run-up model of Shen and Meyer (1963) is used to derive key parameters that indicate the onset of swash saturation and the spectral characteristics of the saturated shoreline motion. These are consistent with recent laboratory data (Baldock et al., 1997) and previous experimental work (Guza and Bowen, 1976; Huntley et al., 1977; Van Dorn, 1978). Simple numerical simulations of swash oscillations are found to reproduce typical features of measured shoreline motions and can accurately describe both the low and high frequency spectral characteristics of the swash zone. This is consistent with recent work by Baldock et al. (1997) which showed that low frequency swash motions may be directly induced by incident wave grouping. A brief review of previous work relating to this study is given in Section 2 of this paper, while Section 3 outlines the theoretical development and the simulation technique. A brief description of the experimental arrangement is provided in Section 4; comparisons between the model and experimental data are presented in Section 5, with final conclusions drawn in Section 6.

2. Previous work

Two different hypothesis are currently used to describe the motion of swash on natural beaches. The first regards swash as driven principally by low frequency infragravity waves which frequently have a cross-shore standing wave structure (Huntley et al., 1977; Guza and Thornton, 1982; Holland et al., 1995; Raubenheimer et al., 1995). Edge waves may also significantly contribute to infragravity energy in the swash (Bowen and Inman, 1971; Guza and Thornton, 1985). The second hypothesis proposes that swash is largely due to bores which collapse at the shoreline and then propagate up the beach face (Shen and Meyer, 1963; Hibberd and Peregrine, 1979; Yeh et al., 1989; Hughes, 1992). The first approach has clearly been identified on mild slope dissipative beaches, whereas the bore hypothesis appears more realistic on steep beaches.

Miche (1951) assumed that the maximum swash amplitude was related to the limiting amplitude of non-breaking standing waves on a plane slope. An increase in the incident wave amplitude above this level would lead to wave breaking and the complete dissipation of the wave energy in excess of that associated with the limiting amplitude; hence the swash is saturated. This is expected to occur when the non-dimensional parameter ε_S reaches some critical value (Iribarren and Nogales, 1949; Miche, 1951):

$$\varepsilon_S = \frac{a_s \omega^2}{g \beta^2} \tag{1}$$

where a_s is the vertical amplitude of the shoreline motion, ω is the angular wave frequency ($2\pi f$—where f is the wave frequency), g the gravitational acceleration and β the beach slope. Experimentally determined values for ε_S vary according to different

researchers; $\varepsilon_S \approx 3 \pm 1$ (Guza and Bowen, 1976), $\varepsilon_S \approx 1.26$ (Battjes, 1974, see Huntley et al., 1977), $\varepsilon_S \approx 2 \pm 0.3$ (Van Dorn, 1978), while the field data of Huntley et al. (1977) suggested a value for ε_S in the range 2 to 3. For monochromatic unbroken standing waves, saturation is predicted to occur when $\varepsilon_S \approx 1$ (Carrier and Greenspan, 1958; Munk and Wimbush, 1969; Raubenheimer and Guza, 1996), a value significantly lower than most of the experimentally determined values. However, to the authors' knowledge, a theoretical value for this parameter has not been previously derived for bores approaching the shoreline. Eq. (1) also suggests that power spectra of shoreline motions will exhibit an f^{-4} roll-off in the saturated band, in agreement with measured data (Sutherland et al., 1976; Huntley et al., 1977), although Guza and Thornton (1982) and Carlson (1984) found an f^{-3} dependency.

However, on steeper beaches (gradients of order 0.1) significant incident short wave energy and wave grouping may remain at the shoreline (Wright and Short, 1984; List, 1991). Indeed, wave grouping may increase shorewards (Kobayashi et al., 1989). Short wave bores may therefore reach the shoreline, driving swash motions at incident wave frequencies (Waddell, 1976; Raubenheimer and Guza, 1996). Shen and Meyer (1963) provide an analytical solution for the shoreline motion following bore collapse and numerical models based on the non-linear shallow water equations have developed from the work of Hibberd and Peregrine (1979), Packwood and Peregrine (1981) and Kobayashi et al. (1989). Raubenheimer et al. (1995) and Raubenheimer and Guza (1996) have shown that such models can accurately describe many features of the swash on natural beaches, although they are fairly computationally intensive. Boussinesq models which allow for frequency dispersion (Freilich and Guza, 1984) can also provide accurate descriptions of surf zone dynamics and swash oscillations (see Madsen et al., 1997). Mase (1988) suggested that the f^{-4} form in the spectral characteristics of the swash might be largely due to the parabolic nature of shoreline motion (see Section 3 below), rather than due to saturation effects. Mase (1988, 1994) also suggested that the low frequency components in the run-up were due to interactions between individual swash events. More recently, Baldock et al. (1997) showed that low frequency swash motions could be directly induced by incident wave groups and were not necessarily due to standing infragravity waves.

In the following sections it is shown that typical spectral characteristics of the swash zone can be predicted and simulated using the simple equations due to Shen and Meyer (1963). Furthermore, Eq. (1) is shown to apply to the bore hypothesis for swash motion and two critical values of ε are derived which indicate the onset of swash saturation. A distinction is also made between the effects of wave grouping that induce low frequency swash motions (Baldock et al., 1997; Mase, 1988) and swash–swash interactions that may generate additional offshore propagating long waves (Watson and Peregrine, 1992).

3. Model formulation

3.1. Monochromatic waves and spectral characteristics

The model for simulating both regular and irregular wave run-up due to bores approaching the shoreline is based on the work of Shen and Meyer (1963) and also

follows on from Mase (1988). At present, for clarity, we assume a plane, hydraulically smooth impermeable beach and an inviscid fluid, although the effects of bed friction could readily be incorporated (e.g., Hughes, 1995). The incident bores are assumed to collapse at the shoreline (Whitham, 1958; Keller et al., 1960), setting the shoreline in motion. The bore collapse involves the rapid conversion of potential energy to kinetic energy, with an associated acceleration of the fluid velocity at the bore front (Shen and Meyer, 1963; Yeh et al., 1989). However, the initial speed of the shoreline, U_o, may be to some extent dependent on the nature of the bore collapse mechanism and hence the incident waves (e.g., uniform bores, undular bores or waves breaking onto the beach as shore breaks). U_o may therefore be written generally as:

$$U_o = C\sqrt{(gH_B)} \tag{2}$$

where H_B is the height of the incident bore at the point of collapse. C is a coefficient which effectively describes the efficiency of the bore collapse and is expected to take a value in the range of 1 to 2 (see below). The subsequent shoreline motion may be described by a simple parabolic equation giving the position of a fluid particle at the front of the swash lens (Shen and Meyer, 1963; Hughes, 1992).

$$X_S(t) = U_o t - \frac{1}{2} g t^2 \sin\beta \tag{3}$$

where X_S is the shoreline position relative to the point of bore collapse and t is the time elapsed since bore collapse. Note that Eq. (3) is simply the classical Newtonian equation describing the motion of a body with constant acceleration. The duration or natural period of the swash, T_S, from the start of the uprush to the end of the backwash is then given by:

$$T_S = \frac{2U_o}{g \sin\beta} \tag{4}$$

However, on all but the steepest slopes, $\sin\beta \approx \beta$ and hence from Eqs. (2) and (4):

$$T_S = \frac{2C\sqrt{gH_B}}{g\beta} \tag{5}$$

The maximum vertical run-up excursion above the point of bore collapse, R, may be found from Eqs. (2) and (3) as:

$$R = \frac{U_o^2}{2g} = \frac{C^2 H_B}{2}. \tag{6}$$

For the simple case where all the potential energy is converted to kinetic energy (Yeh et al., 1989), C takes the theoretical value of 2 and hence $R = 2H_B$. Eq. (5) represents the case where the period of the nearshore incident waves or bores, T_B, is greater than or equal to T_S. Consequently, there is no overlap between sequential swashes. However,

the natural period of the swash is dependent on both the beach slope and the height of the incident bore, Eq. (5). Therefore, increasing H_B while T_B remains constant leads to a new equation which indicates the onset of overlap between sequential swashes when:

$$H_B \geq \frac{g\beta^2}{4C^2f^2} \tag{7}$$

where f is the frequency of the incident bores. Eq. (7) therefore gives the bore height at which the swash just becomes saturated for a given beach slope and incident bore frequency. Substitution of Eq. (7) into Eq. (6) then gives the magnitude of the saturated swash or shoreline motion, R_S, measured from the seaward limit of the swash zone, i.e., the intersection of overlapping swashes or position of maximum run-down.

$$R_S \leq \frac{g\beta^2}{8f^2} \tag{8}$$

Again, Eq. (8) is a new equation giving the magnitude of the saturated swash motion for any particular combination of beach slope and incident wave or bore frequency. Note that since saturation occurs when $T_S \geq T_B$, f in Eq. (8) may be taken to be either the frequency of the incident bores or the fundamental frequency of the parabolic shoreline motion. Alternatively, Eq. (8) may be found from Eq. (3) using symmetry and by considering the amplitude of a parabola of duration T_B. It is also of interest to note that R_S is independent of C, the coefficient describing the efficiency of bore collapse. This suggests that the magnitude or amplitude of the saturated swash motion is likely to be largely independent of the type of bores approaching the shoreline. C does, however, influence the bore height that first results in swash saturation (see Eq. (7)). Consequently, if energy is lost during bore collapse ($C < 2$) then larger incident bores are required to produce swash saturation.

As swash saturation occurs, the mean shoreline position and the seaward limit of the swash zone move shorewards, which may be considered as swash induced set-up in contrast to wave induced set-up in the surf zone. In the absence of frictional or turbulent energy dissipation and additional wave induced set-up in the surf zone, these changes are dependent on the amplitude and frequency of the incoming bores and the beach slope. For regular waves, the change in the vertical elevation of the seaward limit of the swash zone (position of maximum run-down) is simply obtained as the difference between the unsaturated and saturated run-up excursions (Eqs. (6)–(8)). Furthermore, from the properties of a parabola, the mean shoreline position is additionally displaced vertically by $2/3R_S$.

Substitution of Eqs. (7) and (8) into Eq. (1) then allows two new critical values of ε to be determined. The wave or bore amplitude ($H_B/2$) at the position of bore collapse which first produces swash saturation gives ε_B:

$$\varepsilon_B = \frac{g\beta^2}{8C^2f^2}\frac{(2\pi)^2f^2}{g\beta^2} \Rightarrow \varepsilon_B = \frac{(2\pi)^2}{8C^2} \tag{9}$$

For $C = 2$, $\varepsilon_B \approx 1.25$, a value which does not appear to have been derived previously. ε_S, again for broken waves, is given in a similar fashion by the saturated swash amplitude using Eq. (8):

$$\varepsilon_S = \frac{(2\pi)^2}{16} \approx 2.5 \tag{10}$$

This new theoretical value appears consistent with values for ε_S found experimentally, $\varepsilon_S \approx 3 \pm 1$ (Guza and Bowen, 1976), $\varepsilon_S \approx 2 \pm 0.3$ (Van Dorn, 1978), $\varepsilon_S \approx 2$–3 (Huntley et al. (1977)). However, the experiments of Battjes (1974) gave quite a different value; $\varepsilon_S \approx 1.26$ (see Huntley et al., 1977), and this discrepancy between the experimental results remains unresolved.

With the assumption of sinusoidal motion in the surf zone and parabolic motion of the shoreline, both Eqs. (7) and (8) may also be written in terms of their spectral density for comparison with the spectral characteristics of measured data (e.g., Huntley et al., 1977):

$$S_B(f) = \frac{g^2\beta^4}{128C^4f^4}\frac{1}{\delta f} \quad \text{and} \quad S_S(f) = \frac{g^2\beta^4}{720f^4}\frac{1}{\delta f} \tag{11}$$

where δf is a unit frequency ($\delta f = 1$ Hz). It has been drawn to the authors' attention that $S_S(f)$ in Eq. (11) was also derived by Bullock (1968). Note that $S_S(f)$ is predicted to have an f^{-4} roll-off at high frequencies as found previously in both field and laboratory studies (Huntley et al., 1977; Sutherland et al., 1976; Baldock et al., 1997). $S_B(f)$ has a similar roll-off, although this does not imply an f^{-4} roll-off in nearshore sea surface elevation spectra.

However, although Eqs. (7)–(11) predict the characteristic f^{-4} spectral shape, the spectral characteristics of a single parabola also show an f^{-4} dependency (Mase, 1988). For example, following Mase (1988), the vertical component of Eq. (3) may be written in the form:

$$R(t) = \frac{U_o^2}{3g} - \sum_{n=1}^{\infty} \frac{g\beta^2}{2n^2\pi^2f^2}\cos\left(\frac{2n\pi t}{T_S}\right) \tag{12}$$

where $f = n/T_S$, and the spectral density of each harmonic is clearly proportional to f^{-4}. Consequently, the characteristic f^{-4} roll-off in swash spectra appears to be a combination of two processes; firstly the f^{-4} dependence of the saturated swash amplitude at the fundamental swash frequency, Eq. (8) and, secondly, the fact that the amplitudes of the higher harmonic components of parabolic shoreline motions are also proportional to f^{-4} Eq. (12). Note, however, that the combination of the two processes will still result in an f^{-4} roll-off in spectral density.

Finally, by substituting the bore amplitude at the shoreline ($H_B/2$) into Eq. (1), ε_B may be shown to be related to the surf similarity parameter, $\zeta = \beta/\sqrt{H_o/L_o}$, (Iribarren and Nogales, 1949), by $\varepsilon_B = D\pi/\zeta^2$, where D is the ratio of the bore height at the shoreline to the deep water wave height ($D = H_B/H_o$). Since from Eq. (9) the swash

becomes saturated once $\varepsilon_B \geq 1.25$, then unless D/ζ^2 is less than about 0.4, the swash zone will be saturated, typical of the conditions on mildly sloping beaches. However, although the characteristics of the surf zone affect the type of swash motion (Madsen et al., 1997), the present work suggests that this occurs indirectly, largely as a result of the change in the height of the bores reaching the shoreline.

3.2. Irregular wave run-up simulation

Following Mase (1988), the shoreline motion induced by wave groups or random waves may also be simulated using Eq. (3) and the superposition of overlapping parabolas. However, Mase (1988) only used a random sequence of initial velocities (U_o) starting at random time intervals (neither of which were based on physical considerations) to show that the characteristic f^{-4} spectral roll-off could arise from Eq. (1). Here, laboratory measurements of bore heights and their arrival time at the shoreline are used to provide input to a model for run-up due to both wave groups and random waves. Comparisons are then made with the respective measured run-up data and additional simulations based on a Rayleigh p.d.f. for nearshore wave heights (Thornton and Guza, 1983; Baldock et al., 1998).

The numerical simulation is based solely on the bore heights and their arrival time at a fixed position, here taken to be the initial still water shoreline (SWL) (see Section 4 below). This position is taken to be the point of bore collapse for all incident bores, and although this will in general not be the case, the numerical simulation is not overly sensitive to this assumption. The swash model may not be considered entirely predictive, since in the absence of measured data some model for the surf zone is required, although most surf zone models themselves require data at the seaward boundary. However, data at the seaward limit of the swash zone is readily obtained in laboratory studies and also frequently collected during field measurements (e.g., Hughes, 1995) and therefore the present model may be easily applied. Furthermore, simple parametric or probabilistic surf zone models can provide estimates of either r.m.s wave heights or individual wave heights close to the shoreline (e.g., Battjes and Janssen, 1978; Mase and Iwagaki, 1982; Thornton and Guza, 1983; Dally and Dean, 1986; Baldock et al., 1998) and the propagation time across the surf zone for individual waves may be easily estimated from linear theory. One purpose of this paper is therefore to demonstrate that, with input typically available from surf zone models widely used in engineering practice, the simple model presented here is able to predict the overall spectral characteristics of run-up well. This simple model may also highlight the underlying physical run-up processes more readily than full computationally intensive solutions.

Note that wave induced set-up/set-down is not included in the model for several reasons. Firstly, steady set-up/set-down seaward of the swash zone was typically very small for these wave conditions ($O \sim 2$–3 mm). Secondly, in the presence of wave grouping, dynamic set-up occurs in the inner surf zone, which can only be accounted for if the cross-shore wave group structure is known, whereas the present model is solely based on wave conditions close to the shoreline. In addition, for irregular waves, the mean water elevation, and therefore set-up, cannot be uniquely defined shoreward of the position of maximum swash run-down (Brocchini and Peregrine, 1996).

Each individual bore in either a regular or irregular sequence induces a parabolic motion of the shoreline given by Eq. (3), with an amplitude and swash frequency dependent only on the height, H_B, of the incident bore. The shoreline position is then given by the superposition of overlapping parabolas (Fig. 1).

It is important to note that in the model there is no interaction between individual swash events; two or more parabolas do not influence each other or generate additional components in the shoreline motion. However, the superposition process itself may result in additional low frequency harmonics in a frequency analysis of the shoreline motion (see Section 5 below). Baldock et al. (1997) recently showed that these low frequency harmonics in the shoreline motion describe the envelope of the run-up due to individual bores and should not therefore considered to be additional swash motions. In this instance, the term *interaction* used by Carlson (1984) and Mase (1988) to explain the generation of these additional low frequency harmonics by overlapping parabolas is somewhat misleading, since in wave mechanics terms it implies that new harmonic components are generated in the swash zone. The distinction is important since true swash–swash interaction may generate outgoing low frequency waves (Watson and Peregrine, 1992; Watson et al., 1994), whereas superposition of individual overlapping swash events will not. Note that interaction between swash events in the measured data will to some extent be accounted for in the model input, since the backwash from the preceding swash may influence the height of the next incoming bore.

Finally, the superposition method does not explicitly allow for turbulent energy dissipation at the seaward limit of the swash zone. However, energy losses may be accounted for implicitly by varying the coefficient C in Eq. (2). This effectively reduces the efficiency of the bore collapse mechanism and reduces the initial shoreline uprush velocity and, consequently, the maximum uprush elevation Eq. (6). Such a reduction might be expected when an incident bore starts to collapse in the presence of backwash from a previous swash. In the present paper, $C = 1.8$ is found to provide a good representation of the energy losses in the inner surf and swash zone for all cases considered except case R4. For this case (see below) no interaction occurs between sequential swashes and C is taken to be 2. Therefore, although C has a theoretical value, in the model it may be treated as an empirical parameter, similar to empirical friction or bore dissipation coefficients in most existing numerical surf and swash zone models (e.g., Battjes and Janssen, 1978; Packwood and Peregrine, 1981; Kobayashi et al., 1989; Baldock et al., 1998).

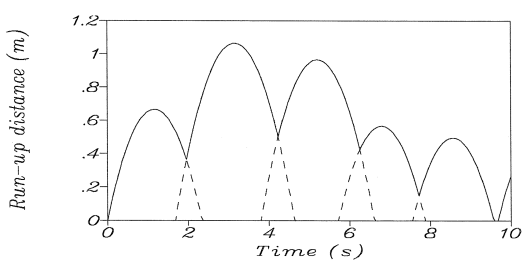

Fig. 1. Simulation of overlapping swash events. ———— Resultant shoreline motion, --- underlying individual swash events.

4. Experimental set-up

4.1. Wave flume

The experiments were carried out in the large wave flume in the Civil Engineering Department at Imperial College. This flume is 50 m long, 3 m wide and was used with a working water depth of 0.9 m (Fig. 2). Waves were generated by a plane bottom-hinged hydraulically-driven wave paddle which can generate both regular waves or random waves up to frequencies of 2 Hz, with simultaneous absorption of short waves reflected from the far end of the flume. A slope (β) of gradient 0.05 starts 32 m from the paddle, rising to 0.1 in the surf and swash zones. The last 6 m of the flume are subdivided into three sections, providing two working sections of width 0.9 m and a central section for access to instrumentation. Wave reflections were comparatively small, with a reflection coefficient measured in the outer surf zone of about 10–15%, although some uncertainties may be introduced due to the presence of wave grouping and non-linear harmonics. Recent work has also suggested that reflection coefficients may increase shoreward (Baquerizo et al., 1997). All data were collected over a bed of glued down sand with a $d_{50} = 0.5$ mm.

4.2. Instrumentation

The vertical elevation of the water surface was measured at the initial SWL position using a modified surface piercing resistance type wave gauge with an absolute accuracy of order ± 1 mm, enabling accurate measurements of the water depth down to 2 mm. The shoreline motion was measured with a resistance type run-up wire fixed 3 mm above the bed. These measurements have a relative accuracy of about 1 mm, but, due to the finite thickness of the component wires, the absolute accuracy was estimated to be of order 20 mm parallel to the bed.

4.3. Wave conditions

The present investigation considers the shoreline motion induced by three regular wave trains, two bichromatic wave groups and three random wave simulations. In the present paper we are primarily concerned with the wave conditions close to the shoreline. These are shown in Table 1, where H_B is the crest elevation of the incident bore measured at the initial SWL. For the random wave cases (Jonswap spectra), H_B is taken as $\sqrt{(8m_o)}$ and for the wave groups H_B is the maximum bore height within the group. This bore height will therefore include any reflected wave energy, which may introduce small errors into the model. The wave groups were generated using two closely spaced harmonics of equal amplitude, resulting in a wave envelope modulated at a frequency, f_m, equal to the frequency spacing. The surf similarity parameter (Iribarren and Nogales, 1949), based on offshore wave heights and deep water wavelength, is

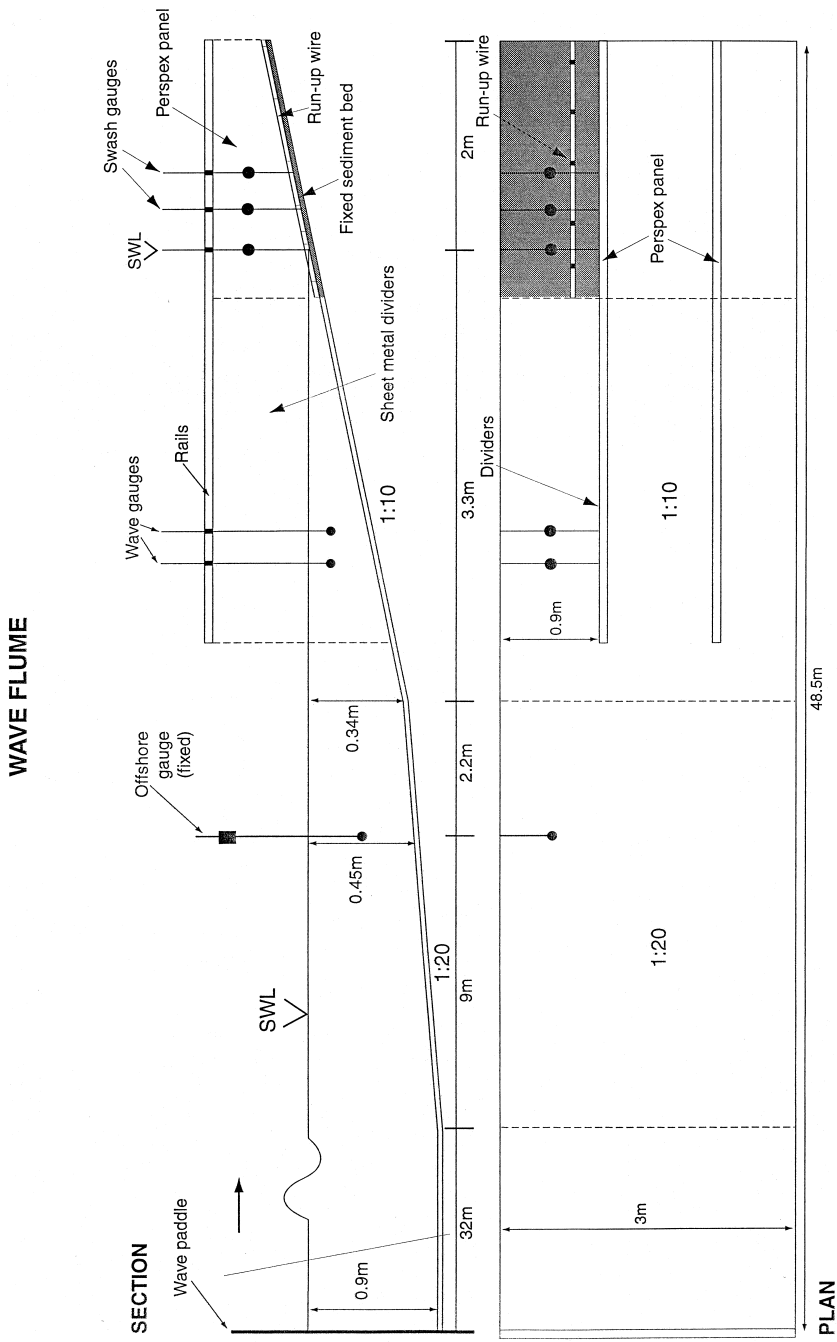

Fig. 2. Wave flume and instrumentation.

Table 1
Experimental wave conditions

Case	T (s), f_m (Hz), T_p (s)	H_B (mm)	H_o / L_o	Surf similarity, ζ_o
R1	1.0	22	0.07	0.37
R2	1.5	40	0.044	0.48
R4	2.5	34	0.01	1
M1	1.5, 0.08	48	0.042	0.49
M2	1.5, 0.15	52	0.042	0.49
J1	1.5	35	0.033	0.55
J2	1.5	34	0.027	0.61
J3	1.0	18	0.031	0.57

typically in the range 0.5 to 0.7, suggesting a combination of spilling and plunging waves within the surf zone.

In the surf zone a combination of incident bound low frequency motions and free long waves propagating seawards and shorewards due to surf beat may be expected. For these wave conditions, Baldock et al. (1997) showed that the amplitude of the total low frequency motion within the inner surf zone was only about 30% of that in the swash zone. Consequently, there was an order of magnitude difference in the low frequency energy levels between the inner surf and swash zones, whereas for standing long waves a much smaller difference would be expected. Baldock et al. (1997) proposed that the large increase in low frequency energy between the seaward limit of the swash zone and that appearing in the run-up was largely due to wave grouping remaining in the inner surf zone. Part of the purpose of the present paper is therefore to show that this effect can be modelled using the simple approach described above.

For the random wave simulations, spectral characteristics were computed using an 8192 point FFT, sampled at 25 Hz and with smoothing over 20 adjacent frequency bins. For the wave groups, spectral estimates were made using a 1024 point FFT, sampled at 25 Hz and with smoothing over 2 adjacent frequencies. Note that in this study both the random wave and wave group data sets may be considered deterministic, and therefore the spectral plots presented in Section 5 do not require the confidence limits associated with stochastic processes.

5. Discussion of results

5.1. Monochromatic waves

Fig. 3a shows a regular sequence of incident bores and their associated shoreline motion for case R4. Note that in this, and similar figures, the vertical elevation of the water surface at the SWL ($x = 0$ and denoted by S_o) is plotted on the right hand scale of the figure and the data have been plotted so that the run-up elevation can also be read on the same scale. The swash in this instance is just on the point of reaching saturation,

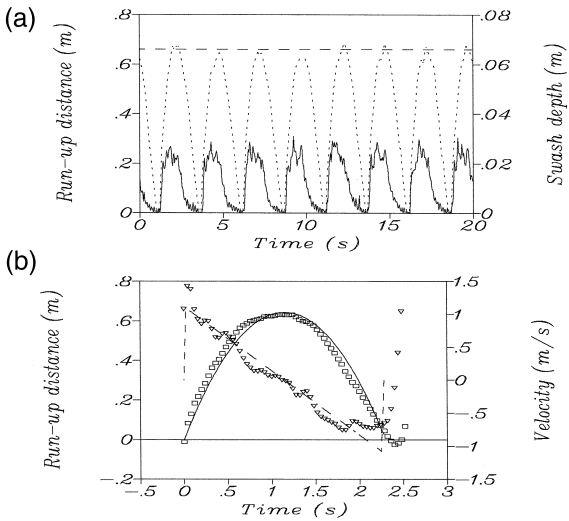

Fig. 3. (a) Run-up and swash depth at $x = 0$, case R4. · · · Run-up wire, ———— S_o (rhs), --- predicted run-up limit Eq. (6). (b) Measured and predicted shoreline motion and velocity, case R4. □ □ □ □ Run-up wire, ———— $X_s(t)$, predicted Eq. (3), ∇∇∇∇ Shoreline velocity, measured (rhs), --- Shoreline velocity, predicted Eq. (3) (rhs).

with T_S fractionally greater than T_B. The maximum run-up height is in good agreement with the theoretical value obtained from Eq. (6), suggesting that frictional effects over this fixed bed are minimal (see also Baldock and Holmes, 1997). Excellent agreement between the measured shoreline position and the predicted position from Eq. (3) with $C = 2$ is shown on Fig. 3b, with negligible run-down below the initial SWL. Eq. (3) also accurately predicts the measured shoreline velocity (plotted on the right hand scale of Fig. 3b), which is consistent with constant acceleration under gravity.

Examples of saturated swash under monochromatic conditions are shown on Fig. 4a and Fig. 5a for cases R2 and R1, respectively. For case R2, although the incident bores are larger than the previous case, significant overlap occurs between sequential swashes and the amplitude of the swash motion has reduced significantly as the bore frequency has been increased. For case R1, the incident bore frequency has increased sufficiently to reduce the shoreline motion even further and in both cases the magnitude of the shoreline motion is in reasonable agreement with Eq. (8).

Fig. 4b and Fig. 5b show the simulations of the shoreline motion for these two cases ($C = 1.8$). In each instance, the input to the simulation is simply the bore height measured at the SWL, indicated on the figures. Note that due to instabilities inherent in relatively steep Stokes' waves, both cases show some deviation from uniform bore conditions. Although the details of the shoreline motion are not reproduced exactly, the overall behaviour of the model is consistent with the measured data, particularly for case R2. However, for case R1, because the degree of overlap between sequential swashes is so extreme, increasing the generation of turbulence at the seaward limit of the swash zone, the assumptions in the model start to become invalid.

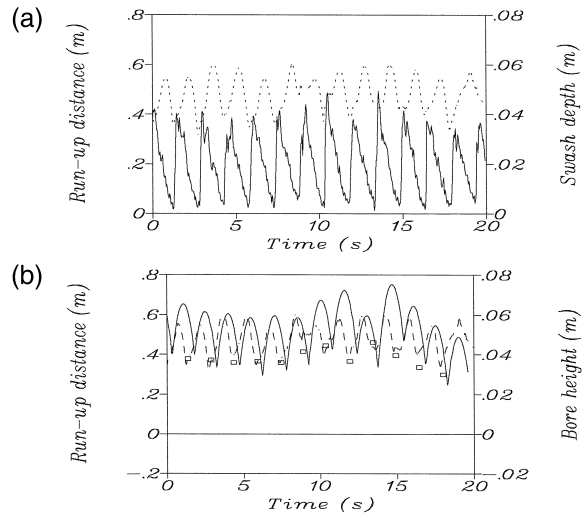

Fig. 4. (a) Run-up and swash depth at $x = 0$, case R2. · · · Run-up wire, ———— S_o (rhs). (b) Measured and simulated run-up, case R2. --- Run-up wire, ———— simulated, □ □ □ □ H_B (rhs).

5.2. Wave groups

Fig. 6a and b show similar simulations for the two wave groups, cases M1 and M2, again with $C = 1.8$. The combination of incident wave swash and a slow modulation of the shoreline position due to the wave grouping is well described by the simulation.

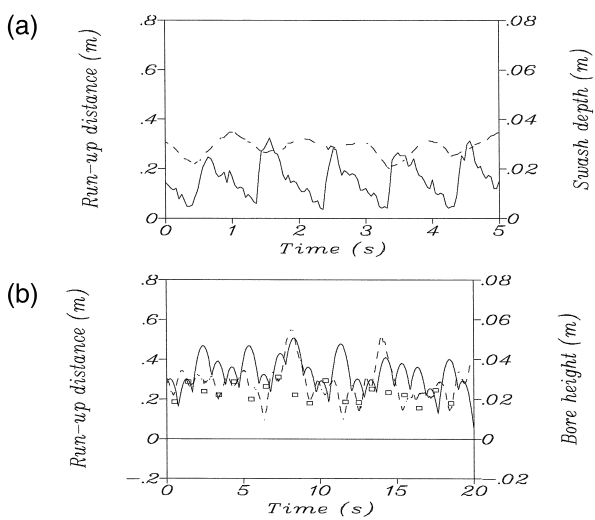

Fig. 5. (a) Run-up and swash depth at $x = 0$, case R1. · · · Run-up wire, ———— S_o (rhs). (b) Measured and simulated run-up, case R1. --- Run-up wire, ———— simulated, □ □ □ □ H_B (rhs).

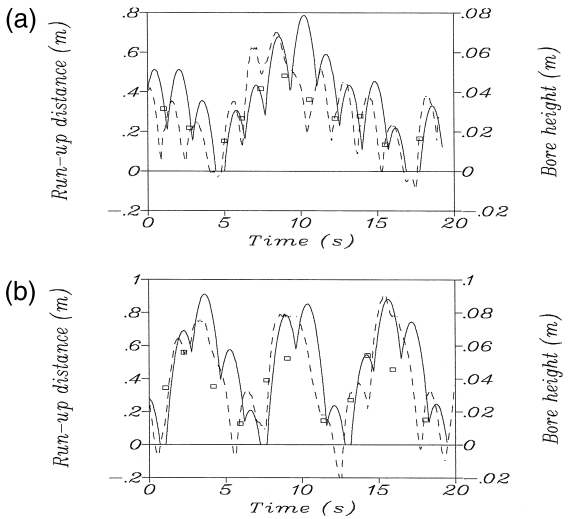

Fig. 6. (a) Measured and simulated run-up, case M1. --- Run-up wire, ———— simulated, □ □ □ □ H_B (rhs). (b) Measured and simulated run-up, case M2. --- Run-up wire, ———— simulated, □ □ □ □ H_B (rhs).

However, again, small details of the motion may be incorrectly reproduced. For example, for case M1, the simulation produces a swash event starting at $t = 9$ s, whereas the measured data shows that this event was nearly totally prevented by the preceding backwash. A similar effect occurs at $t = 4$ s for case M2. Nevertheless, given the simplicity of the model, the agreement between the measured and simulated data is striking.

It should be noted that at present the model does not attempt to reproduce run-down below the initial SWL. This is because the input conditions for the model were only available at this fixed position. Consequently, the calculations have been curtailed at the SWL to avoid spurious infinite shoreline accelerations arising due to the jump from the run-down position back to the SWL for the next incident bore. If both the bore height and position of bore collapse had been, or were, available (i.e., from video analysis, Hughes, 1995), then run-down below the SWL could readily be included. However, since the degree of run-down below the SWL is minimal for the present data sets, only minor errors are introduced by this discrepancy.

Comparisons of the spectral characteristics of the measured and simulated data sets are shown on Fig. 7a and b. For both cases M1 and M2, the spectral characteristics of the measured and simulated data are very similar, with both main spectral peaks predicted accurately. Therefore, since there is no direct low frequency input to the run-up model, the correct prediction of the dominant spectral peak at the group frequency, f_m, clearly suggests that the low frequency harmonics in the run-up are predominantly due to wave grouping and not due to long waves. Furthermore, the good agreement between the measured and predicted spectral characteristics suggests that energy losses due to turbulence (which are not included in the model) have little effect

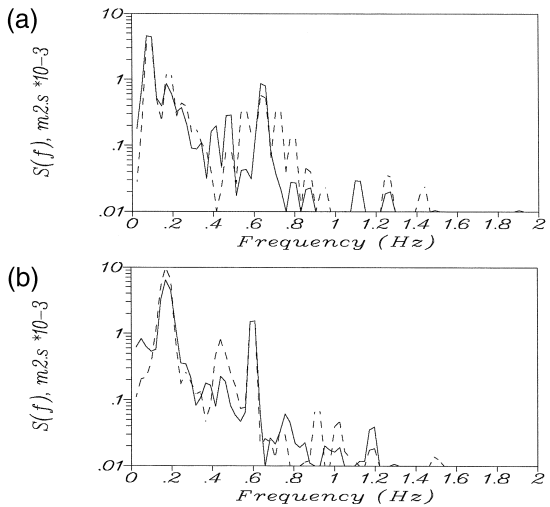

Fig. 7. (a) Power spectra of measured and simulated run-up, case M1. --- Measured run-up, ———— simulated run-up. (b) Power spectra of measured and simulated run-up, case M2. --- Measured run-up, ——— simulated run-up.

on the characteristics of the shoreline motion. This is because these energy losses predominately occur seaward of the instantaneous shoreline through the interaction of the incoming bore with the preceding backwash. In the present model, this can be accounted for by varying the coefficient C in Eq. (2).

5.3. Random waves

Comparisons between the measured and simulated shoreline motion for two random wave cases, J1 and J3, are shown on Figs. 8 and 9, respectively ($C = 1.8$). Again, although the simulation does not exactly reproduce the details of the shoreline motion, the overall pattern is similar. Furthermore, the accuracy of the simulation does not diminish over the length of the data set (compare Figs. 8a,b and 9a,b). The shoreline motion is therefore largely driven by individual incident bores and does not exhibit a cumulative increase in additional harmonics due to true swash–swash interactions. In addition, no accumulation of long wave energy (not absorbed by the wave paddle) is apparent, which suggests that outgoing long wave energy is small. The simulation also highlights particular features of the measured data. For example, on Fig. 8a, two swash events overlap at $t \approx 55$ s. This is only just visible in the measured data, where the run-down is held up by the uprush due to the second of the two incoming bores. A similar effect occurs at $t \approx 333$ s (Fig. 8b) and, in general, overlapping swash events tend to be smoothed in the measured data. This is to be expected, since the model does not allow for explicit swash–swash interaction, whereas in reality this will occur. Nevertheless, the lack of interaction in the model has little overall effect on the simulated spectral characteristics (see below). Note that the algorithm used to determine

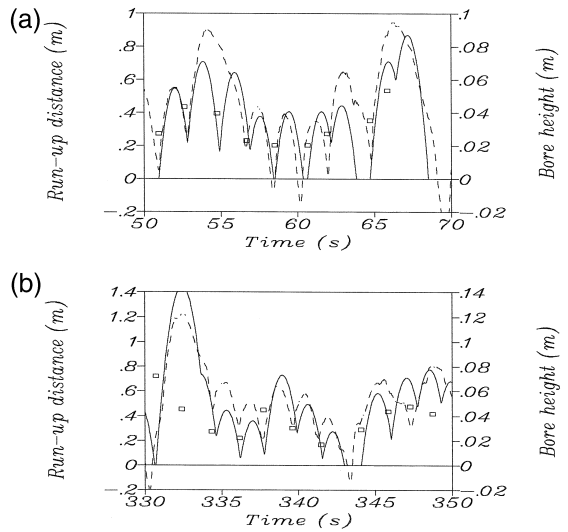

Fig. 8. (a) Measured and simulated run-up, case J1. --- Run-up wire, ———— simulated, □ □ □ □ H_B (rhs). (b) Measured and simulated run-up, case J1. --- Run-up wire, ———— simulated, □ □ □ □ H_B (rhs).

the incident bore height from the vertical elevation of the water surface at the SWL (S_o) occasionally misses an incident bore due to noise in the data record (e.g., at $t \approx 315$ s on Fig. 9b).

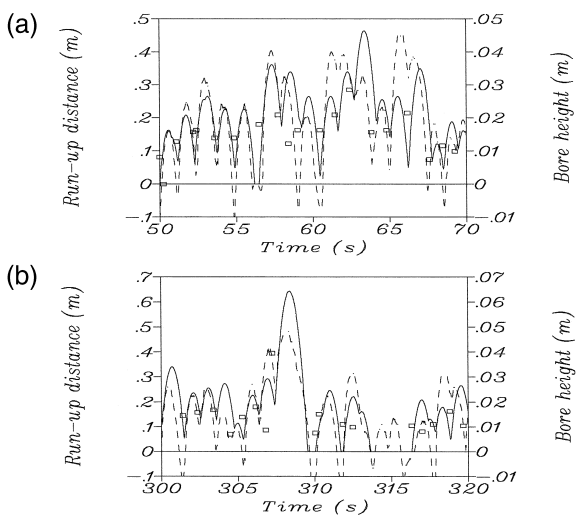

Fig. 9. (a) Measured and simulated run-up, case J3. --- Run-up wire, ———— simulated, □ □ □ □ H_B (rhs). (b) Measured and simulated run-up, case J3. --- Run-up wire, ———— simulated, □ □ □ □ H_B (rhs).

Fig. 10a and b compare the spectral characteristics of the measured and simulated data for cases J1 and J3, respectively. In each case, both spectra are dominated by low frequency harmonics and the agreement is generally good, particularly for case J1. The discrepancy between the measured and simulated data for case J3 appears largely due to the neglect of run-down below the SWL in the model. This is generally greater for case J3 (compare Figs. 8 and 9). However, the excellent agreement at low frequencies again shows that the model is capable of reproducing the effects of wave grouping on swash run-up. Therefore, since the model can simulate the low frequency characteristics of swash motion with no direct long wave input, the assumption that the dominance of infra-gravity energy in typical field data is largely due to standing long waves or edge waves must be questioned, as also noted by Mase (1988).

Very similar spectral characteristics result from a simulation using a Rayleigh p.d.f. to describe the nearshore bore heights (Thornton and Guza, 1983; Baldock et al., 1998). The simulation was carried out using a random sequence of bores with the same r.m.s. bore height as case J1 and the same mean bore period (T_z), randomly distributed between $T_z \pm 0.5$ s. It is important to note that in this case there is no direct or indirect low frequency long wave input to the model, the input is simply a sequence of bores of varying height and period. Fig. 11a shows a short segment of the simulated shoreline motion and the spectral characteristics of this simulation are compared to those of case J1 on Fig. 11b. The similarities between the measured data and purely simulated data is very striking, particularly at low frequencies, although the spectral peak at the incident bore frequency is slightly more pronounced. This appears to be due to the choice of the frequency bandwidth of the incident bores. Consequently, with a simple model to describe nearshore wave heights on a steep beach, where significant short wave energy may remain in the inner surf zone, it appears possible to accurately simulate the resulting swash energy levels.

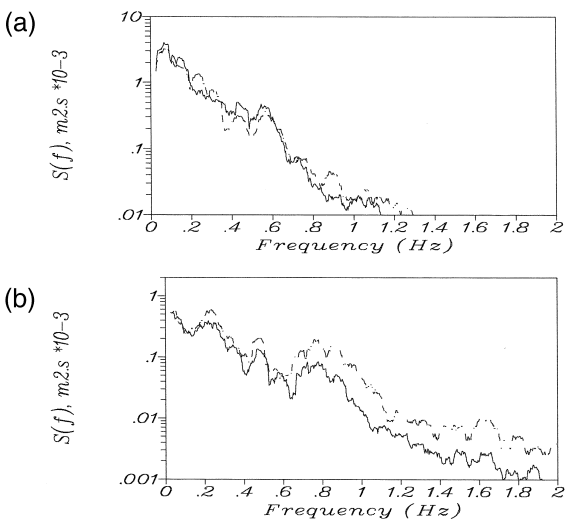

Fig. 10. (a) Power spectra of measured and simulated run-up, case J1. --- Measured, ———— simulated. (b) Power spectra of measured and simulated run-up, case J3. --- Measured, ———— simulated.

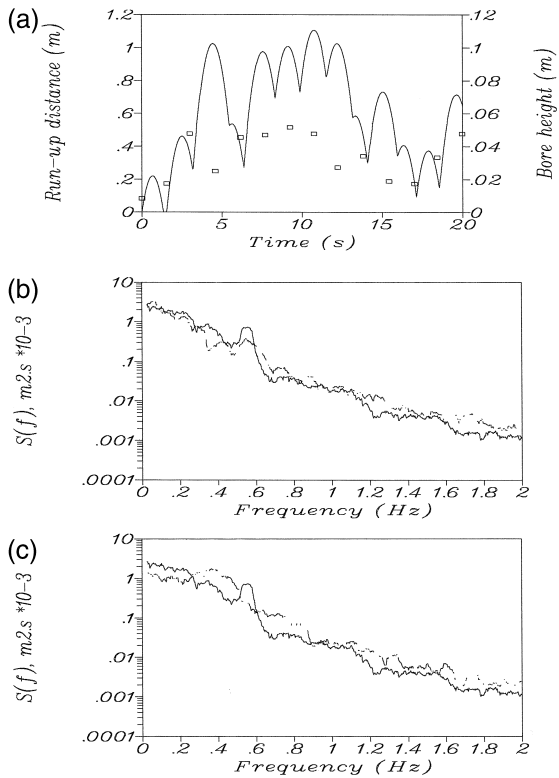

Fig. 11. (a) Simulated run-up, Rayleigh p.d.f. for nearshore bore heights. ———— Simulated run-up, □ □ □ □ H_B (rhs). (b) Power spectra of measured and simulated run-up, case J1 compared to Rayleigh p.d.f. for nearshore bore heights. --- Measured, ———— simulated. (c) Power spectra of simulated run-up with and without swash overlap, Rayleigh p.d.f. ———— with overlap, – · – without overlap.

Carlson (1984) and Mase (1988) proposed that the low frequency components in the swash were due to swash–swash interaction, leading to the generation of additional run-up components. However, in both the simulations of Mase (1988) and the present model there is no mechanism for true swash–swash interactions. These components therefore arise, in part, due to the overlap of sequential swash events. However, it is not necessary to have overlap between sequential swash events in order for these low frequency components to arise in a harmonic analysis of the shoreline motion. For example, Fig. 11c compares the spectral characteristics of the previous simulation using the Rayleigh p.d.f. with a simulation using an identical sequence of incident bores but with no overlap between sequential swashes, i.e., the run-up due to each bore does not commence until the end of the preceding backwash. Note that again there is no direct or indirect low frequency long wave input to the model. This comparison shows that about 80% of the low frequency energy is due to the variability in wave height and bore period, with the remainder arising from the overlap of sequential swashes. Furthermore, in both cases, the low frequency energy exceeds that at the incident bore frequency. The

good agreement between the simulated and measured data for cases J1 and J3 (Fig. 10a,b and Fig. 11b) clearly suggests that the predominant part of the apparent low frequency energy in the swash is simply due to the variable height of the incident bores and hence wave grouping in the nearshore.

This is consistent with recent work by Baldock et al. (1997), who showed that low frequency energy in the swash could be directly linked to modulations in the offshore wave height. However, it is important to note that these effects will only occur if wave grouping remains in the nearshore. If the inner surf zone is totally saturated, i.e., wave grouping is totally destroyed, then low frequency energy in the swash is likely to be due to free incident long waves (e.g., Holland et al., 1995; Raubenheimer et al., 1995). Further work is, however, required on wave groupiness in the nearshore, since List (1991) shows that significant wave height variation is found even in a saturated surf zone.

5.4. High frequency spectral characteristics

Mase (1988) originally showed that a parabolic shoreline motion will result in an f^{-4} spectral roll-off in the higher harmonics (Eq. (12)). This is further illustrated on Fig. 12a, which shows the power spectrum of a simulation of the run-up for case R4 (see Fig. 3a). However, in Section 3 it was shown that the energy of the saturated swash motion will also roll-off at f^{-4}, with the spectral density given by Eq. (11), and both effects will contribute to the measured or simulated spectral characteristics. Comparisons between the power spectra of the measured data, simulated data and Eq. (11) in the high frequency region are shown on Fig. 12b–d. For case J1, both the measured data and simulated data are in excellent agreement with Eq. (11). Furthermore, if the energy in the saturated frequency band were due to cross-shore standing waves, then $\varepsilon_S \approx 1$(Carrier and Greenspan, 1958; Raubenheimer and Guza, 1996) and the measured saturated spectral density would be nearly an order of magnitude smaller than that predicted by Eq. (11). Similarly good agreement is found with Eq. (11) for the simulation using a Rayleigh p.d.f. for the nearshore bore heights (Fig. 12c) and for cases J2 and J3 (Fig. 12d). These spectra all show characteristics typical of field data from both steep and mildly sloping beaches (e.g., Huntley et al., 1977; Guza and Thornton, 1982; Raubenheimer et al., 1995; Raubenheimer and Guza, 1996), which suggests that the simple model proposed in Section 3 could be applicable to field conditions.

Finally, using Eq. (11) and given the spectrum of the water surface elevation just seaward of the swash zone, the frequency at which the swash first becomes saturated should be predictable. Accordingly, when the spectral density of the nearshore water surface elevation, S_o, exceeds $S_B(f)$, the spectral density of the swash should exceed $S_S(f)$. Furthermore, once swash saturation occurs, the spectral density of the water surface elevation (S_o) and the run-up will tend to converge. Conversely, below the saturation frequency the spectral density of the swash should be less than that given by Eq. (11). This is illustrated on Fig. 13a and b for cases J1 and J3, respectively. Fig. 13a shows that saturation is predicted to start at about 0.45 Hz. However, in this case there is a spectral valley in the run-up spectrum at about 0.5 Hz, and therefore the measured spectral density does not exceed $S_S(f)$ at exactly this frequency. For case J3, the

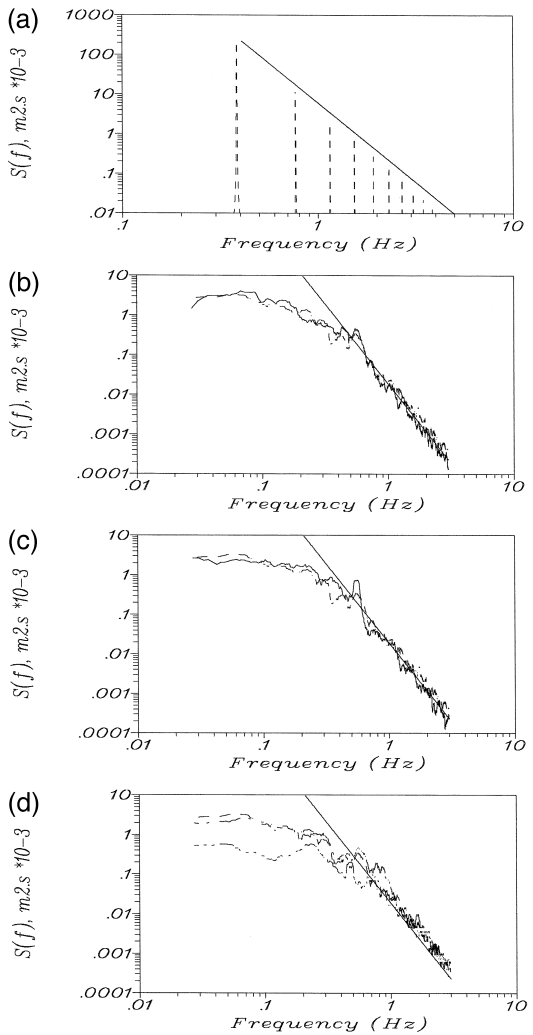

Fig. 12. (a) Power spectrum of simulated parabolic run-up, case R4. --- Simulated, ———— f^{-4} roll-off. (b) Power spectra of measured and simulated run-up, case J1. --- Measured, ———— simulated, ———— $(g^2\beta^4/720f^4)(1/\delta f)$. (c) Power spectra of measured and simulated run-up, case J1 compared to Rayleigh p.d.f. for nearshore bore heights. --- Measured, ———— simulated, ———— $(g^2\beta^4/720f^4)(1/\delta f)$. (d) Power spectra of measured run-up, cases J1–J3. · · · J1, – · – J2, --- J3, ———— $(g^2\beta^4/720f^4)(1/\delta f)$.

saturation frequency appears better estimated, with both $S_B(f)$ and $S_S(f)$ crossing the measured spectral density plots at the same frequency (0.65 Hz). In addition, the predicted saturation frequencies calculated from Eq. (7) using the r.m.s. bore heights given in Table 1 are 0.46 and 0.65 for cases J1 and J3, respectively, also in excellent agreement with those predicted by Eq. (11) and the spectral density plots. Therefore, at least for these cases, the saturation frequency of random wave swash can be accurately

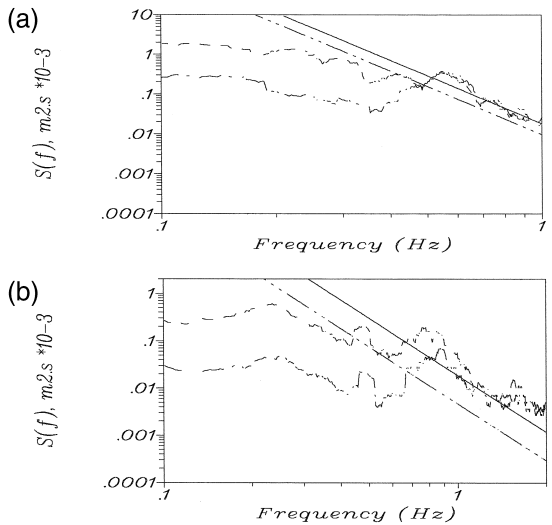

Fig. 13. (a) Power spectra and predicted saturation levels, case J1. --- Run-up, – · – S_o, ———— $(g^2\beta^4/720f^4)(1/\delta f)$, – · – $(g^2\beta^4/128C^4f^4)(1/\delta f)$. (b) Power spectra and predicted saturation levels, case J3. --- Run-up, – · – S_o, ———— $(g^2\beta^4/720f^4)(1/\delta f)$, – · – $(g^2\beta^4/128C^4f^4)(1/\delta f)$.

predicted using monochromatic swash parameters. Further analysis of existing field data is required to determine if this is in general the case, although the good agreement between the predicted values of ε_S from Eq. (10) and the value obtained by Huntley et al. (1977), $\varepsilon_S \approx 2$–3, suggests that it is probable.

6. Conclusions

Experimental data on swash oscillations have been presented for regular waves, wave groups and random waves and the data compared to numerical simulations and theoretical predictions. The non-dimensional parameter (Miche, 1951)

$$\varepsilon = \frac{a\omega^2}{g\beta^2} \tag{13}$$

is re-derived using the equations for the shoreline motion proposed by Shen and Meyer (1963). For monochromatic short wave bores collapsing at the shoreline, two new theoretical values of ε are found: $\varepsilon_B \approx 1.25$, which gives the amplitude of the incident bore which first results in swash saturation, and $\varepsilon_S \approx 2.5$, which describes the vertical amplitude of the shoreline motion at saturation. Theoretical predictions describing the onset and spectral density of random wave saturated swash conditions are in good agreement with the laboratory data, and are also consistent with previous data (e.g., Huntley et al., 1977). This therefore suggests that the typical spectral characteristics of random wave swash can be predicted from monochromatic parameters.

The numerical simulations, based solely on the height and arrival time of short wave bores at a fixed position (here the initial SWL), provide a good overall description of the shoreline motion induced by wave groups and random waves. Furthermore, although the model does not include swash–swash interaction, and therefore some of the finer details of the shoreline motion are not accounted for, comparisons between the measured and simulated data sets suggest that such interactions have little overall effect on the swash. Indeed, the spectral characteristics of the measured and simulated data sets show excellent agreement for both the wave groups and the random wave cases.

The numerical simulations have been shown to reproduce the dominant low frequency energy found in spectral analysis of the laboratory run-up data, and which is also typically observed in field data. This is despite the fact that there is no direct low frequency long wave input to the model. Furthermore, simulations based on a Rayleigh p.d.f. for nearshore bore heights, which have no direct or indirect low frequency input, also show very good agreement with the measured data. Hence, at least for these experimental conditions, the low frequency components in a harmonic analysis of the swash have been shown to be largely due to the effects of variable incident bore height and not free incident long waves. In addition, overlap between sequential swashes is not the principal reason for the appearance of this low frequency energy, wave grouping is in itself sufficient. This implies that the dominance of low frequency energy in shoreline run-up spectra, typically observed in field data from steep and mildly sloping beaches, is likely to be due to both wave group effects and free incident long waves. The importance of each process to the shoreline motion will therefore depend on conditions in the surf zone.

Acknowledgements

The authors gratefully acknowledge the financial support of the UK Engineering and Physical Sciences Research Council. TB was supported for part of this work by the European Commission through the MAST III programme, SASME project, contract no: MAS3-CT97-0081.

References

Baldock, T.E., Holmes, P., 1997. Swash hydrodynamics on a steep beach. Proc. Coastal Dynamics'97, Plymouth, UK, 784–793.

Baldock, T.E., Holmes, P., Horn, D.P., 1997. Low frequency swash motion induced by wave grouping. Coastal Engineering 32, 197–222.

Baldock, T.E., Holmes, P., Bunker, S., Van Weert, P., 1998. Cross-shore hydrodynamics within an unsaturated surf zone. Coastal Engineering 34, 173–196.

Baquerizo, A., Losada, M.A., Smith, J.M., Kobayashi, N., 1997. Cross-shore variation of wave reflection from beaches. J. Waterway, Port, Coastal and Ocean Eng. ASCE 123, 274–279.

Battjes, J.A., 1974. Surf similarity. Proc. 14th Int. Conf. Coastal Eng. ASCE, New York, 1419–1438.

Battjes, J.A., Janssen, J.P., 1978. Energy loss and setup due to breaking of random waves. Proc. 16th Int. Conf. Coastal Eng. ASCE, New York, 569–588.

Bowen, A.J., Inman, D.L., 1971. Edge waves and crescentic bars. J. Geophys. Res. 76, 8662–8671.
Brocchini, M., Peregrine, D.H., 1996. Integral flow properties of the swash zone and averaging. J. Fluid Mech. 317, 241–273.
Bullock, G.N., 1968. A study of the run-up of irregular waves on uniform slopes. PhD thesis, University of Southampton, UK, 203 pp.
Carlson, C.T., 1984. Field studies of run-up on dissipative beaches. Proc. 19th Int. Conf. Coastal Eng., ASCE, New York, 399–414.
Carrier, G.F., Greenspan, H.P., 1958. Water waves of finite amplitude on a sloping beach. J. Fluid Mech. 4, 97–109.
Dally, W.R., Dean, R.G., 1986. Transformation of random breaking waves on surf beat. Proc. 20th Int. Conf. Coastal Eng., ASCE, New York, 109–123.
Freilich, M.H., Guza, R.T., 1984. Non-linear effects on shoaling surface gravity waves. Phil. Trans. R. Soc. Lond. A 311, 1–41.
Guza, R.T., Bowen, A.J., 1976. Resonant interaction for waves breaking on a beach. Proc. 15th Int. Conf. Coastal Eng., ASCE, New York, 560–579.
Guza, R.T., Thornton, E.B., 1982. Swash oscillations on a natural beach. J. Geophys. Res. 87, 483–491.
Guza, R.T., Thornton, E.B., 1985. Observations of surf beat. J. Geophys. Res. 90, 3162–3172.
Hamm, L., Madsen, P.A., Peregrine, D.H., 1993. Wave transformation in the nearshore: a review. Coastal Engineering 21, 5–39.
Hibberd, S., Peregrine, D.H., 1979. Surf and run-up on a beach: a uniform bore. J. Fluid Mech. 95, 323–345.
Holland, K.T., Raubenheimer, B., Guza, R.T., Holman, R.A., 1995. Run-up kinematics on a natural beach. J. Geophys. Res. 100 (C3), 4985–4993.
Hughes, M.G., 1992. Application of a non-linear shallow water theory to swash following bore collapse on a sandy beach. J. Coastal Res. 8, 562–578.
Hughes, M.G., 1995. Friction factors for wave uprush. J. Coastal Res. 11, 1089–1098.
Huntley, D.A., Guza, R.T., Bowen, A.J., 1977. A universal form for shoreline run-up spectra?. J. Geophys. Res. 82, 2577–2581.
Iribarren, C.R., Nogales, C., 1949. Protection des ports. Sect. 2, comm. 4, 17th Int. Nav. Cong., Lisbon, 31–80.
Keller, H.B., Levine, D.A., Whitham, G.B., 1960. Motion of a bore over a sloping beach. J. Fluid Mech. 7, 302–316.
Kobayashi, N., DeSilva, G.S., Watson, K.D., 1989. Wave transformation and swash oscillation on gentle and steep slopes. J. Geophys. Res. 94, 951–966.
List, J.H., 1991. Wave groupiness variations in the nearshore. Coastal Engineering 15, 475–496.
Madsen, P.A., Sorensen, O.R., Schaffer, H.A., 1997. Surf zone dynamics simulated by a Boussinesq type model: Part 2. Surf beat and swash oscillations for wave groups and irregular waves. Coastal Engineering 32, 289–319.
Mase, H., 1988. Spectral characteristics of random wave run-up. Coastal Engineering 12, 175–189.
Mase, H., 1994. Uprush–backrush interaction dominated and long wave dominated swash oscillations. In: Isaacson, M., Quick, M. (Eds.), Proc. Int. Symp. Waves—Physical and Numerical Modelling. UBC, Vancouver, 1, 316–325.
Mase, H., Iwagaki, Y., 1982. Wave height distributions and wave grouping in surf zone. Proc. 18th Int. Conf. Coastal Eng., ASCE, New York, 58–76.
Miche, R., 1951. Exposes a l'action de la houle. Ann. Ponts et Chaussees 121, 285–319.
Munk, W.H., Wimbush, M., 1969. A rule of thumb for wave breaking. Oceanology 9, 56–99.
Packwood, A.R., Peregrine, D.H., 1981. Surf and run-up on beaches: models of viscous effects. University of Bristol, School Mathematics Rep. No. AM-81-07.
Raubenheimer, B., Guza, R.T., 1996. Observations and predictions of run-up. J. Geophys. Res. 101, 25575–25587.
Raubenheimer, B., Guza, R.T., Elgar, S., Kobayashi, N., 1995. Swash on a gently sloping beach. J. Geophys. Res. 100, 8751–8760.
Shen, M.C., Meyer, R.E., 1963. Climb of a bore on a beach 3: run-up. J. Fluid Mech. 16, 113–125.
Sutherland, A.J., Sharma, J.N., Shemdin, O.H., 1976. Wave run-up on a simulated beach. Proc. 15th Int. Conf. Coastal Eng., ASCE, New York, 752–766.

Thornton, E.B., Guza, R.T., 1983. Transformation of wave height distribution. J. Geophys. Res. 88, 5925–5938.

Van Dorn, W.G., 1978. Breaking invariants in shoaling waves. J. Geophys. Res. 83, 2981–2987.

Waddell, E., 1976. Swash–groundwater–beach profile interactions. In: Davis, R.A., Etherington, R.L. (Eds.), Beach and nearshore sedimentation. SEPM Spec. Publ., 24, 115–125.

Watson, G., Peregrine, D.H., 1992. Low frequency waves in the surf zone. Proc. 23rd Int. Conf. Coastal Eng., ASCE, New York, 818–831.

Watson, G., Barnes, T.C.D., Peregrine, D.H., 1994. The generation of low frequency waves by a single wave group incident on a beach. Proc. 24th Int. Conf. Coastal Eng., ASCE, New York, 776–790.

Whitham, G.B., 1958. On the propagation of shock waves through regions of non-uniform area or flow. J. Fluid Mech. 4, 337–360.

Wright, L.D., Short, A.D., 1984. Morphodynamic variability of surf zones and beaches: a synthesis. Mar. Geol. 56, 93–118.

Yeh, H.H., Ghazali, A., Marton, I., 1989. Experimental study of bore run-up. J. Fluid Mech. 206, 563–578.